RC-LACE stay report

TKE-based mixing length in TOUCANS

Mario Hrastinski

Supervised by: Jan Mášek and Radmila Brožková

22/10 - 2/11/2018

1 Introduction

During the previous stay [1] it was found that stability-dependent conversion (SDC) from the output of TKE-based mixing-length formulations (L_{TKE}) to Prandtl type mixing length (l_m) leads to violation of Monin-Obukhov similarity theory (MOST), even for weak deviations from neutrality. This, together with the fact that TOUCANS characteristic length scales (L_K, L_ϵ and L) are necessarily larger than z, left l_m as the only possible option to which L_{TKE} can be (directly) assigned. However, we are still left with two degrees of freedom: i) the choice of an averaging operator for L_{up} and L_{down}, i.e. the way how L_{TKE} is computed and ii) the way of including κ into l_m to ensure matching with MOST in the surface layer. During the process of adding shear effects to Bougeault-Lacarrère (BL89) formulation (cf. [2] and [3]) a bug in discretization of the corresponding integral (cf. [1] or check below in Ch. 2) was found. This bug results in overestimation of mixing in stable stratification, while in unstable stratification it leads to slower accumulation of available energy. Since the original TOUCANS method of discretization is valid with the assumption of a constant Brunt-Väisälä frequency profile during integration path, we implemented another method (theta2) that is more general and consistent with [2] and [3]. One of the main tasks during this stay is to compare these methods and to see whether the inclusion of moist effects through unbugged version of the original discretization method improves the model performance in cloudy atmospheric boundary layer (ABL).

2 Discretization of the Bougeault-Lacarrere (BL89) integral

2.1 Theoretical background

Originally, the BL89 method is based on:

$$\int_{z}^{z+L_{up}} \frac{g}{\theta_v(z')}[\theta_v(z') - \theta_v(z)]dz' = e(z) \tag{1}$$

$$\int_{z-L_{down}}^{z} \frac{g}{\theta_v(z')}[\theta_v(z) - \theta_v(z')]dz' = e(z) \tag{2}$$

where L_{up} and L_{down} are upwards and downwards vertical displacement, z and z' are heights of the starting level and parcel's actual point, θ_v is virtual potential temperature and e(z) is TKE at the starting level. It should be noted here that θ_v in denominator of (1) and (2) is a function of z', which is not highlighted neither in [2], nor in [4].

On the other hand BL89 formulation in TOUCANS is based on the Brunt-Väisälä frequency approach [4]:

$$\int_{z}^{z+L_{up}} N_v^2(z' - z)dz' = e(z) \tag{3}$$

$$\int_{z-L_{down}}^{z} N_v^2(z - z')dz' = e(z) \tag{4}$$

where N_v^2 can be either "dry" (bvd method; virtual temperature effect included) or moist (bvm method; including phase changes). Both in (2) and (4), there is a constraint on downwards displacement, i.e. $L_{down} \leq z$. During the transition from (1)-(2) to (3)-(4) it is assumed that N_v^2 is constant in the vertical direction and that (z'-z) $\rightarrow$ 0. In practical implementation of BL89 formulation in TOUCANS, (z'-z) factor in (3) and (4) is (by mistake) replaced with dz (layer thickness), which can be done only for the starting layer. If integration path covers several layers, (z'-z) factor is significantly higher than dz. This results in overestimation of vertical displacement in stable stratification (smaller value of integral - longer integration path), while in unstable stratification it leads to slower accumulation of available energy (smaller value of integral - less addition to the right-hand side). One of the goals here is to evaluate the impact of above mentioned assumptions, as well as to check whether the moist unbugged version of (3)-(4) can improve the model performance in cloudy PBL.

2.2 Experiments in the diagnostics mode

Before further modifications, the latest code version is phased from CY38t1trlx-op8 to CY43t2-op2 of the ALADIN system at CHMI. The diagnostics of L_{up} and L_{down} is performed within the reference formulation (Geleyn-Cedilnik; cf. eq. (108) in [5]), i.e. the forecast evolution is not affected by different discretization methods of the BL89 integral (eq. (1)-(2) or (3)-(4)). This allows us to estimate the pure impact of different discretization methods on calculation of L_{up} and L_{down}, as well as the effect of different averaging operators on computation of l_m within the same discretization method.

Regarding the latter one, the code is now simplified. Since the SDC approach is abandoned due to above mentioned reasons (introduction), there is no need to transfer additional variables (stability functions) from **ACMRIP** to **ACMIXELEN** subroutine. l_m is now made directly proportional to L_{TKE}, whereby we will test following dependencies:

$$l_m = \kappa \cdot min(L_{up}, L_{down}) \tag{5}$$

$$l_m = \kappa \cdot min(z, L_{TKE}) \tag{6}$$

$$l_m = min(\kappa z, L_{TKE}) \tag{7}$$

where L_{TKE} is, for the time being, obtained by using following averaging operators:

$$L_{TKE} = \sqrt{L_{up} \cdot L_{down}} \tag{8}$$

$$L_{TKE} = \frac{2L_{up} \cdot L_{down}}{L_{up} + L_{down}} \tag{9}$$

Note that l_m vs. L_{TKE} dependencies are created to ensure the near-surface κz limit of l_m. Due to the constraint imposed on L_{down}, l_m obtained from (5)-(7) should behave similarly near the surface. However, significant differences are expected in upper layers where κz factor increases and l_m becomes proportional to L_{TKE}, L_{up} or L_{down}. Also note that (7) is the only pure BL89 related solution above the κz layer, as (5) and (6) are affected by global κ scaling. Any other constant above that layer is equally (un)justified and (un)wanted.

The impact of a bug in the "bvd" discretization method is shown on Figure 1. for the case of summer convection. As expected, it is huge near the surface and for an upwards displacement.

During relatively stable night conditions the unbugged version of the "bvd" method provides results that are quite similar to those of the "theta2" method. However, during the unstable daily conditions there are significant differences between the methods, i.e. the "bvd" method underestimates an upwards displacement. This is attributed to the assumption of a constant N_v^2 profile, both for "bvd" and "bvm" methods. On the other hand, for a downwards displacement the impact of a bug is largest in a narrow region where maximum is achieved. This is a direct consequence of a constraint imposed on L_{down}.

The same conclusions are also valid for the "bvm" method, except for the fact that there is a secondary maximum within the cloud layer (Figure 2.). It can be also seen that the inclusion of moist effects increases both L_{up} and L_{down}, except near the surface where the latter one is constrained.

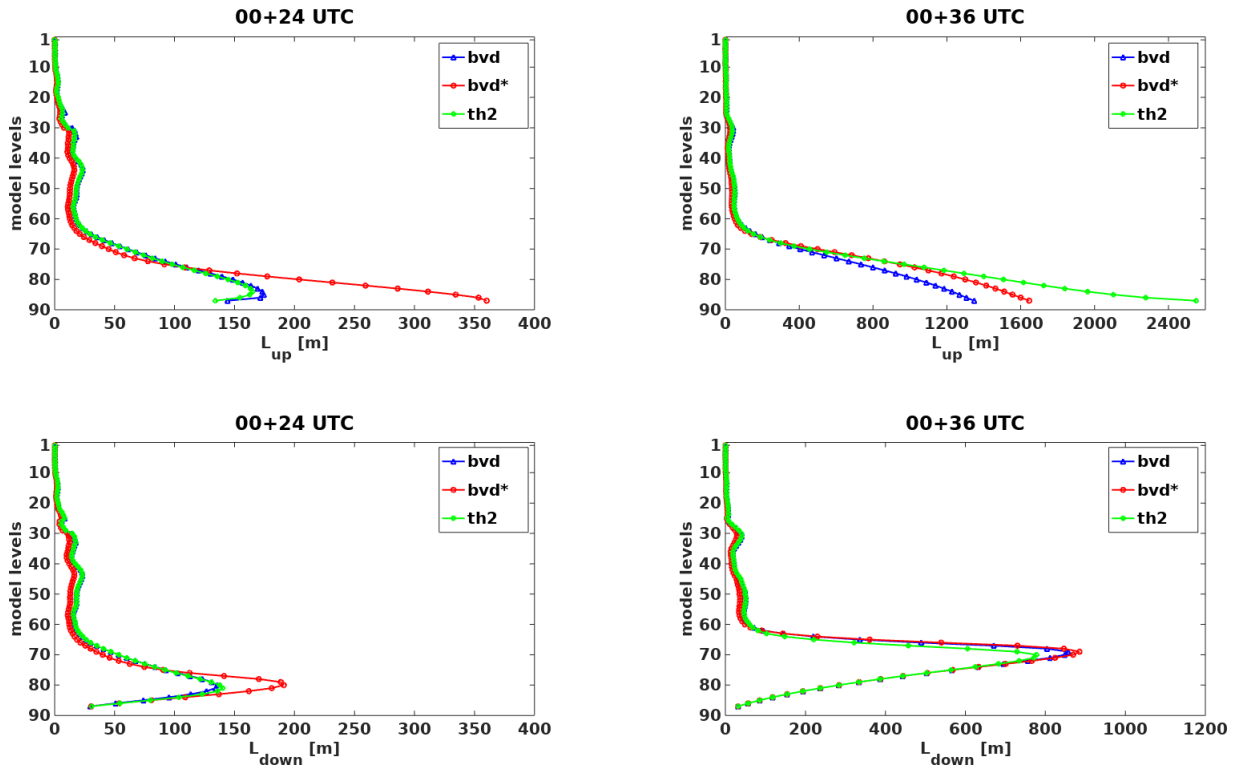

Figure 1: Comparison of averaged L_{up} and L_{down} obtained by three different discretization methods: i) unbugged "dry" Brunt-Väisälä frequency method (bvd), ii) bugged "dry" Brunt-Väisälä frequency method (bvd*) and iii) theta 2^{nd} order accuracy method (th2). Notice a different scale on the x-axis.

However, vertical displacements do not (directly) effect the forecast evolution. For this reason we need to evaluate the impact of methods used to compute l_m from both L_{up} and L_{down}; eq. (5)-(7). The impact of two dependencies which use global κ scaling is shown on Figure 3., while

the third one will be shown later on, together with experiments in the prognostic mode. At the time, only the geometric averaging operator for computation of L_{TKE} is considered.

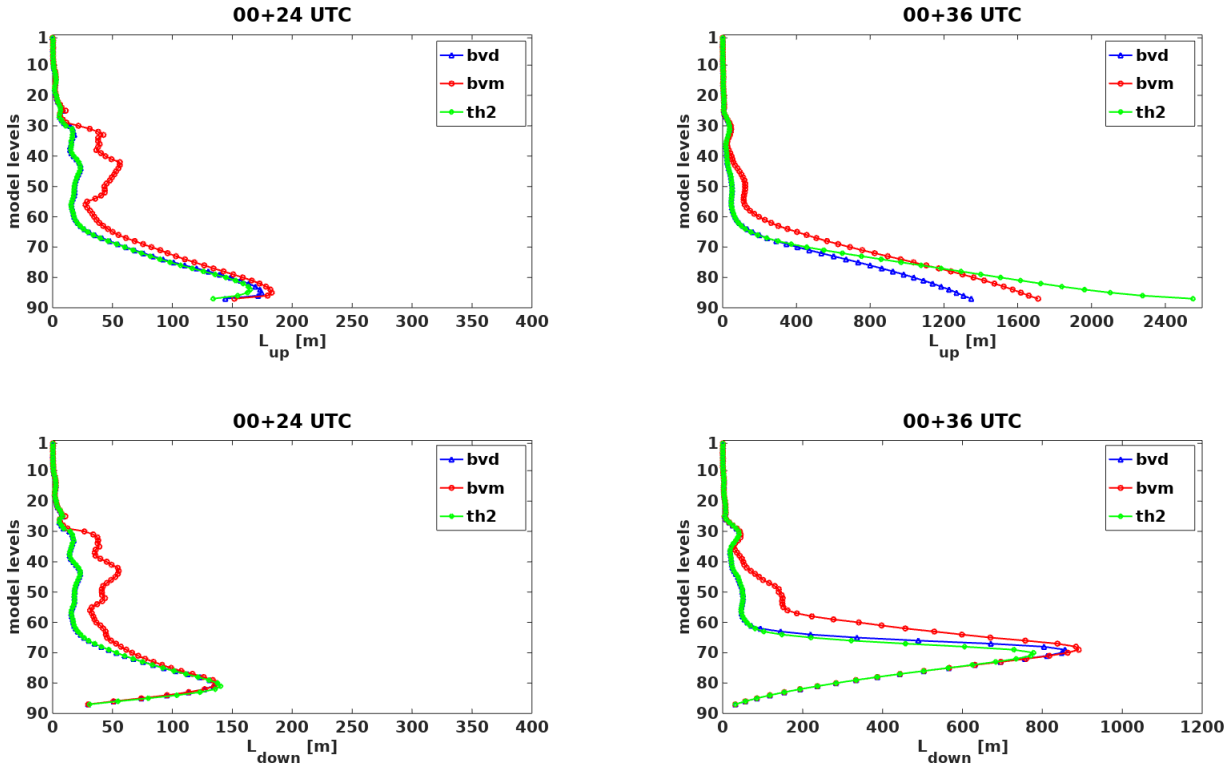

Figure 2: Comparison of avaraged L_{up} and L_{down} obtained by three different discretization methods: i) unbugged "dry" Brunt-Väisälä frequency method (bvd), ii) unbugged moist Brunt-Väisälä frequency method (bvm) and iii) theta 2^{nd} order accuracy method (th2). Notice a different scale on the x-axis

Despite significant differences between the near-surface values of L_{up} for "theta2" and "bvd" methods, l_m is almost identical for both (Figure 3.), i.e. L_{up} contribution is practically negligible there. Higher up, the values of both displacements are similar. Hence, there is no much difference whether they are averaged or minimum of them is taken to compute l_m. As for vertical displacements, the impact of third discretization method ("bvm") on computation of l_m is also significant, except near the surface where κz limit is imposed.

So far we found that: i) both "dry" discretization methods provide similar values of l_m (despite significant differences for L_{up}), ii) the impact of moist processes on computation of l_m is significant above the κz layer, particularly above the maximum of mixing and iii) the role of an averaging operator for l_m is small above its maximum. Keeping this in mind, our focus in prognostic mode experiments will be on the impact of moist processes and type of κ scaling.

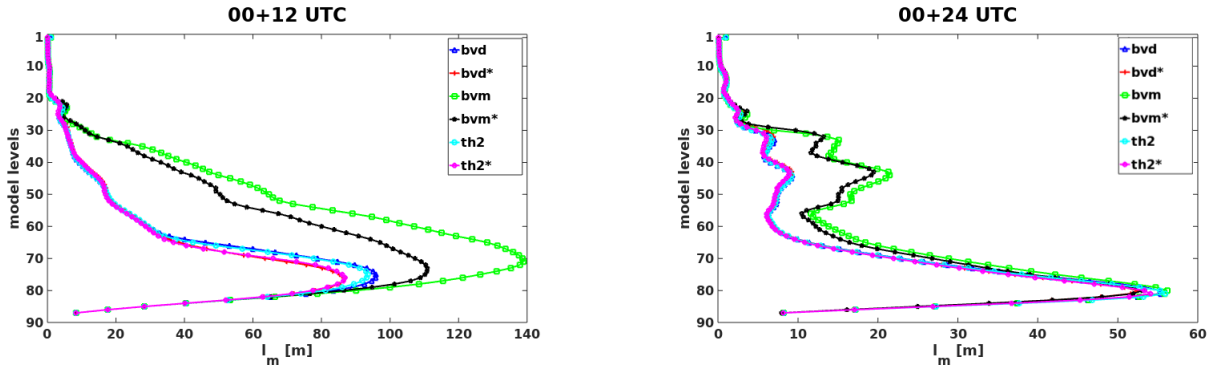

Figure 3: Comparison of l_m obtained by combination of two averaging operators (eq.5 - with * and eq.6 - without *) and three discretization methods: i) unbugged "dry" Brunt-Väisälä frequency method (bvd), ii) unbugged moist Brunt-Väisälä frequency method (bvm) and iii) theta 2^{nd} order accuracy method (th2). Notice a different scale on the x-axis.

3 Experiments with the new conversion approach

A set of experiments using different discretization methods (for BL89 integral) and averaging operators (for vertical displacements) was launched for two cases: i) winter case: 15-17^{th} January 2017 and ii) summer case: 28-30^{th} June 2017. The onset of both cases was related to multiple low pressure systems that were formed over North Sea/Eastern Europe and produced significant precipitation for that particular part of the year. This was especially the case for the later one, where multiple convection events were triggered even before and after the period we study here. Contrary, the former one ended with dry anticyclonic weather related to the cold airflow from Eastern Europe.

As expected, both dry discretization methods perform similary for both cases, with negligible differences in verification scores. For this reason, we will only show the results for the "theta2" method as it is more general and consistent with the original [2]. Unfortunately, the inclusion of moist processes produced unstable simulations for the summer case, no matter which averaging operator or κ scaling type we utilized. After several tests, the simulations were finally stabilized by introduction of additional constant (α=0.75) which multiplies L_{TKE} in (6). This was combined with the namelist switch (or more precisely by setting the large enough decorrelation depth) which turns on maximum random cloud overlap instead of exponential-random (in microphysics only). However, this is not a direction we want to follow. Moist simulations for the winter case were stable, but with mixed verification scores. For these reasons, the "bvm" method is put on a side for the time being.

3.1 Winter case: 15-17th January 2017

Here we present the results of selected simulations for the winter case (Figures 4-8.). The impact of discretization method and κ scaling type on averaged mixing length profile is shown on Figure 4. As it was stated before, two "dry" methods do not differ significantly. However, depending on the type of κ scaling, differences are huge. Especially during the day, when both regions of below and above the maximum of l_m are affected. Compared to the reference, both local and global κ-scaled mixing length have larger amplitude of a daily cycle, as well as the vertical variation of a height where the maximum occurs. Contrary, the amplitude of a daily cycle is rather small for the reference. However, the depth of a layer before which l_m drops to its asymptotic value is larger during the day. It is expected that these daily variations, observed in profiles of the TKE-based l_m, will result in reduction of forecast errors.

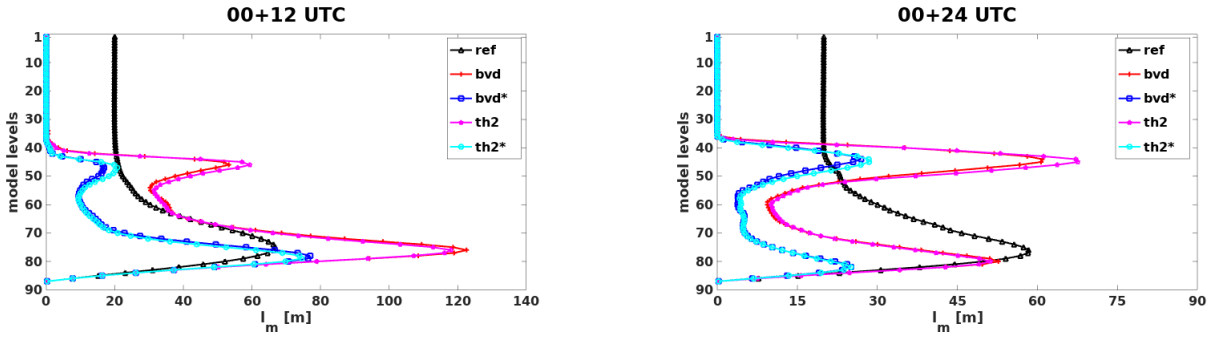

Figure 4: Comparison of the reference l_m and those obtained by combination of two averaging operators (eq.6 - with * and eq.7 - without *) and two discretization methods: i) unbugged "dry" Brunt-Väisälä frequency method (bvd) and ii) theta 2^{nd} order accuracy method (th2). Notice a different scale on the x-axis.

The BIAS and RMSE of temperature (t2m) and relative humidity (rh2m) at 2 [m] AGL for the reference and BL89 method with global κ scaling are shown of Figure 5. The scores for local κ scaling were significantly worse and for conciseness reasons will not be shown here. As it can be seen, the warm t2m bias of the reference is almost completely reduced within our experiment. This is related to decrease of negative bias of cloudiness (Figure 6.), especially the low and to some extent the middle (not shown here). Concerning the rh2m, the BIAS in our experiment is improved only during the night. For all analyzed parameters, the RMSE is reduced as well.

The observed improvements in forecast scores are related to strengthening of the near-surface turbulent diffusion of heat (Figure 7.) and moisture (Figure 8.), wherein the layer where this occurs is thinner for the later one. Stronger turbulent diffusion led to triggering of several feedback effects, resulting in significant decrease of the t2m. On the other hand, the rh2m daily variations are smaller and seem to be very sensitive to response of other processes on small variations in turbulence intensity, thus affecting the forecast BIAS.

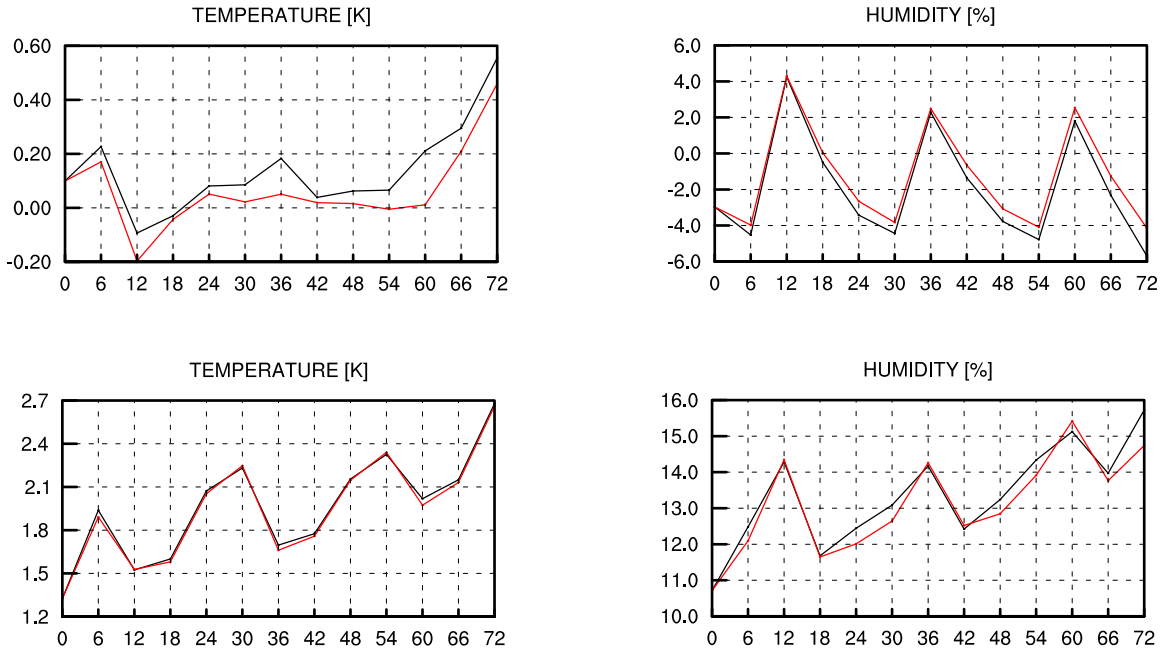

Figure 5: BIAS (upper pannels) and RMSE (lower pannels) of temperature (left) and relative humidity (right) at 2m AGL for the winter case.

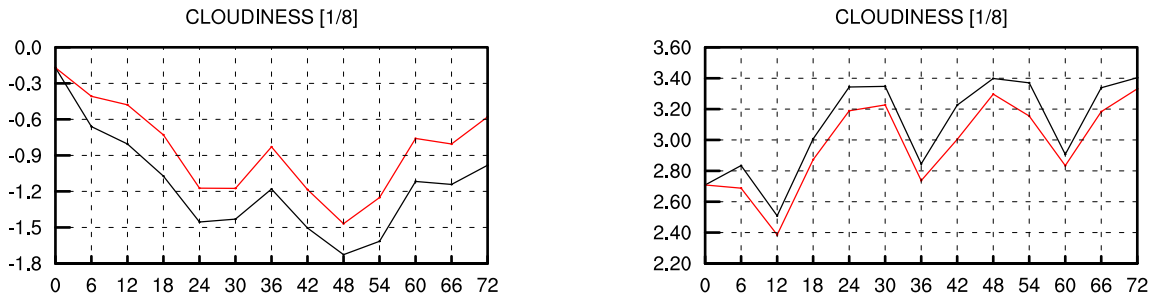

Figure 6: BIAS (left) and RMSE (right) of cloudiness for the winter case.

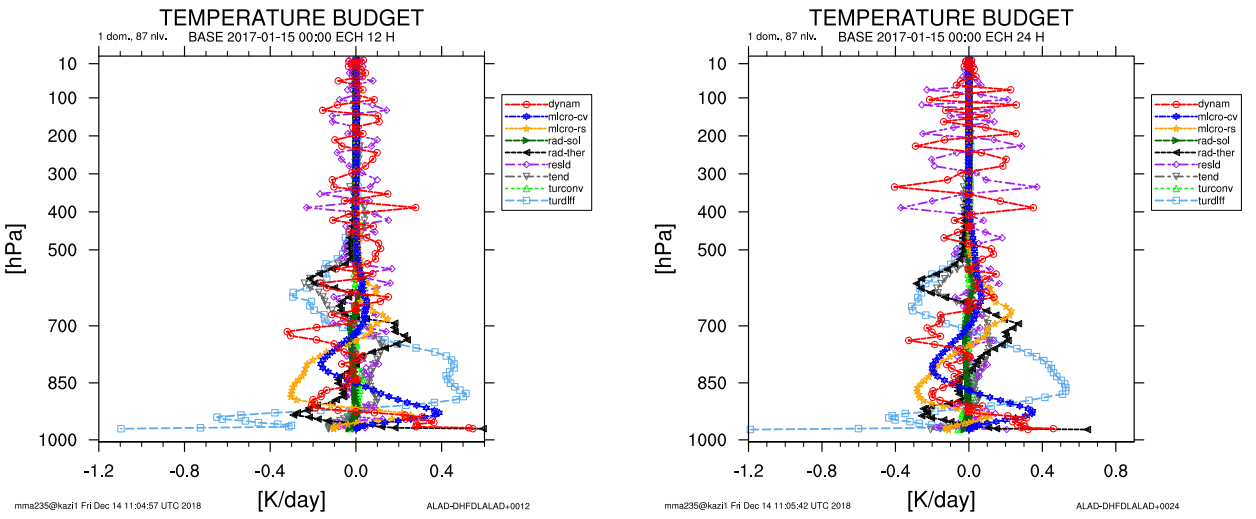

Figure 7: Impact on averaged temperature budget for the winter case at +12 hours (left) and +24 hours (right). "+" sign indicates that particular process is stronger in the reference, while "-" sign indicates that particular process is stronger in the experiment.

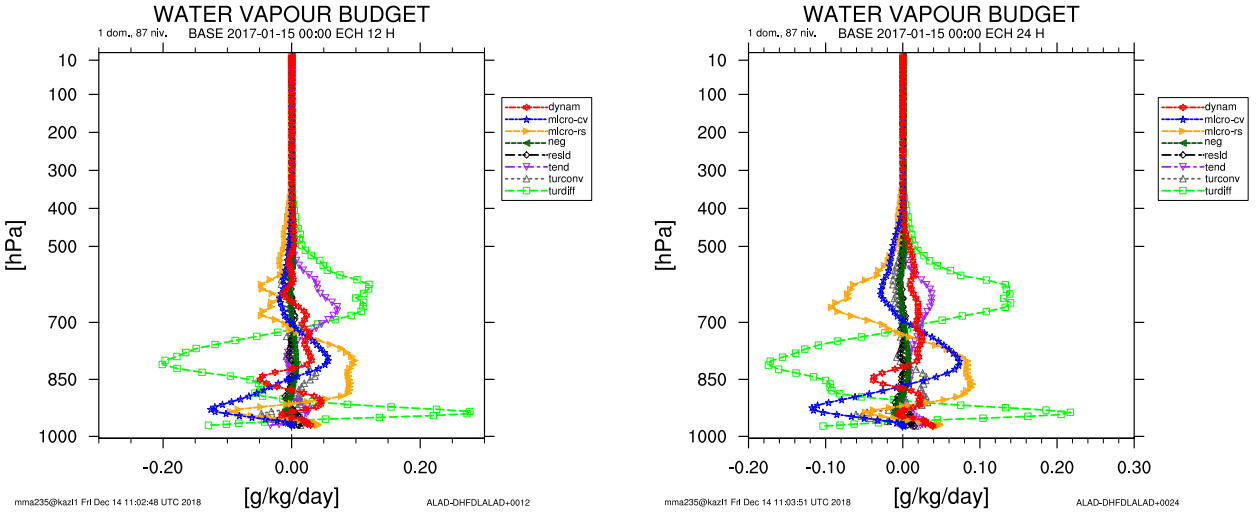

Figure 8: Impact on averaged water vapour budget for the winter case at +12 hours (left) and +24 hours (right). "+" sign indicates that particular process is stronger in the reference, while "-" sign indicates that particular process is stronger in the experiment.

Most of the upper layer scores are very similar to the reference, except for those at around 850 [hPa] pressure level (not shown here). There the scores for the experiment are slightly worse. Possible cause and solution will be discussed within the conclusion part.

3.2 Summer case: 28-30th June 2017

Here we present the results of selected simulations for the summer case (Figures 9-14.). The impact of discretization method and κ scaling type on averaged mixing length profile is shown on Figure 9. As it was stated for the winter case (and before that), two "dry" methods do not differ significantly. On the other hand, the impact of the type of κ scaling is significant. Especially during the day, when local scaling produces enormous mixing throughout the first $\approx$ 5 [km] of troposphere (left panel of Figure 9.). Compared to the reference, both local and global κ-scaled mixing length have larger amplitude of a daily cycle, as well as the vertical variation of height where the maximum occurs. It is expected that these daily variations, observed in profiles of the TKE-based l_m, will result in reduction of forecast errors.

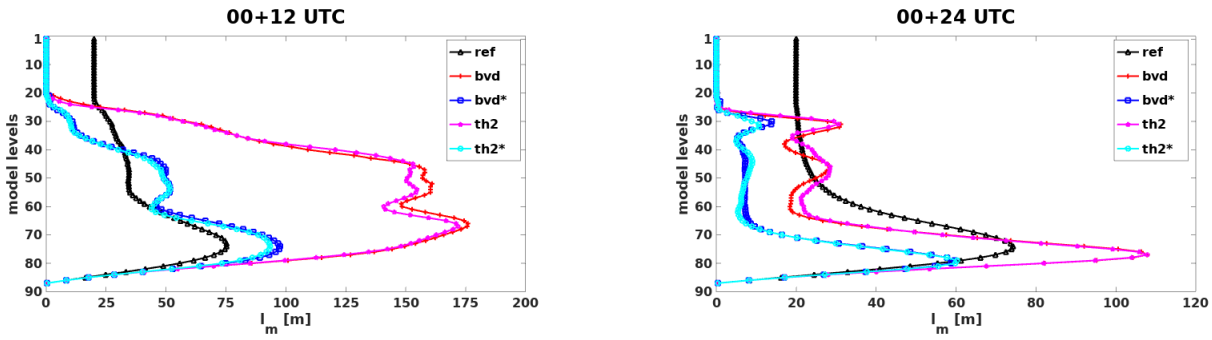

Figure 9: Comparison of the reference l_m and those obtained by combination of two averaging operators (eq.6 - with * and eq.7 - without *) and two discretization methods: i) unbugged "dry" Brunt-Väisälä frequency method (bvd) and ii) theta 2nd order accuracy method (th2). Notice a different scale on the x-axis.

The BIAS and RMSE of temperature (t2m) and relative humidity (rh2m) at 2 [m] AGL for the reference and BL89 method with global κ scaling are shown of Figure 10. As for the winter case, the scores for local κ scaling were significantly worse and will not be shown here for conciseness reasons. The bias of t2m is now greatly increased, i.e. t2m is colder than the reference, which is related to decrease of the negative bias of cloudiness (Figure 11.). The later is primarily result of increase in middle cloudiness and to much lesser extent of low and high cloudiness (not shown here). Unlike the winter case, the BIAS of rh2m is now improved during the afternoon. The RMSE for both t2m and rh2m is comparable to the reference, while for cloudiness it is clearly improved.

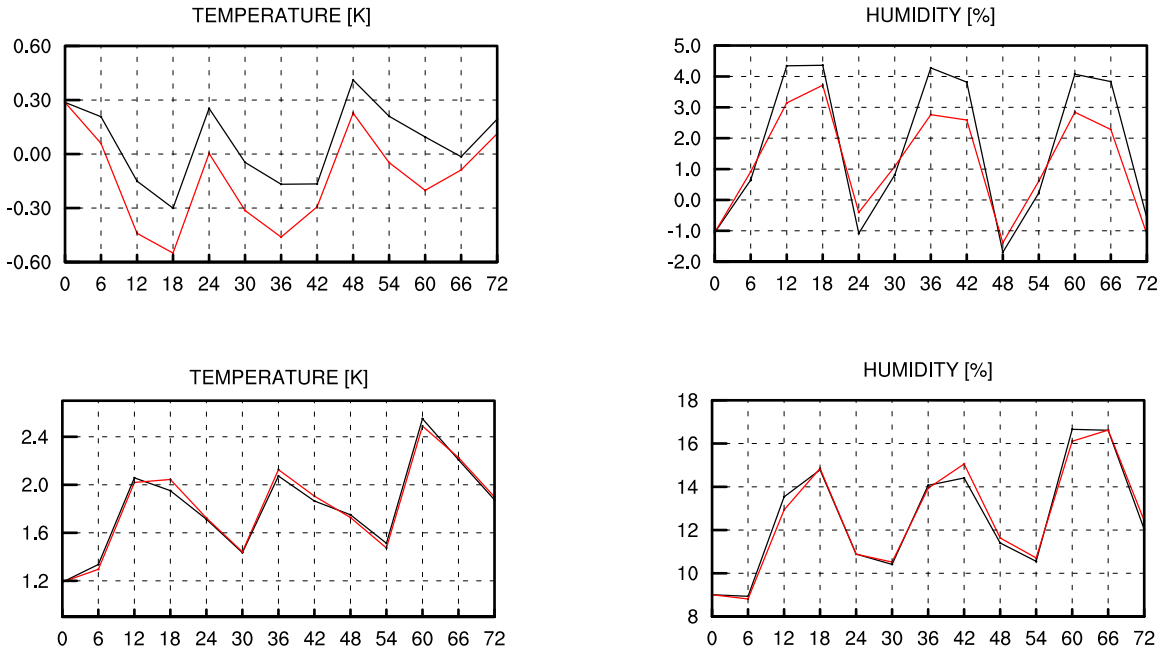

Figure 10: BIAS (upper panels) and RMSE (lower panels) of temperature (left) and relative humidity (right) at 2 m AGL for the summer case.

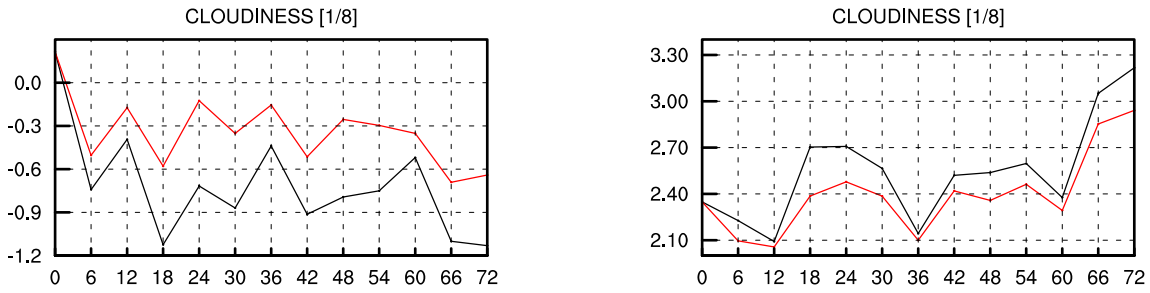

Figure 11: BIAS (left) and RMSE (right) of cloudiness for the summer case.

The observed cooling near the surface (t2m) is related to relative strengthening (compared to the reference) of turbulent diffusion of heat (Figure 12.). However, there are some differences between the day and night. Relatively stronger turbulence, accompanied with weaker compensating processes (dynamics in particular), results in large negative tendency during the day (relative to the reference). During the night when turbulence decreases and compensating processes become stronger, the negative amplitude of temperature tendency decreases. As a result of all these differences the experiment is always colder, but during the night this means that the forecast is improved as positive bias of the reference is decreased.

Regarding the rh2m, we expect significant impact of differences in surface evapotranspiration (Figure 13.). As it can be seen, there is more income of moisture from the corresponding processes within the experiment, and in particular during the night. During the day this excess of moisture is raised by very intense turbulence into upper layers, which results in a large negative tendency of water vapour within a relatively deep layer near the surface (Figure 14.). The impact is seen on the bias of rh2m, which is reduced in the experiment. However, this deficit of near-surface heat and moisture means that there is not enough fuel for convection. During the night when turbulent diffusion of moisture weakens, the compensating processes become stronger (e.g. dynamics) which results in decreasing of the relative difference in tendency. At the screen level, where evapotranspiration is stronger (in experiment), this results in a slight increase of moisture.

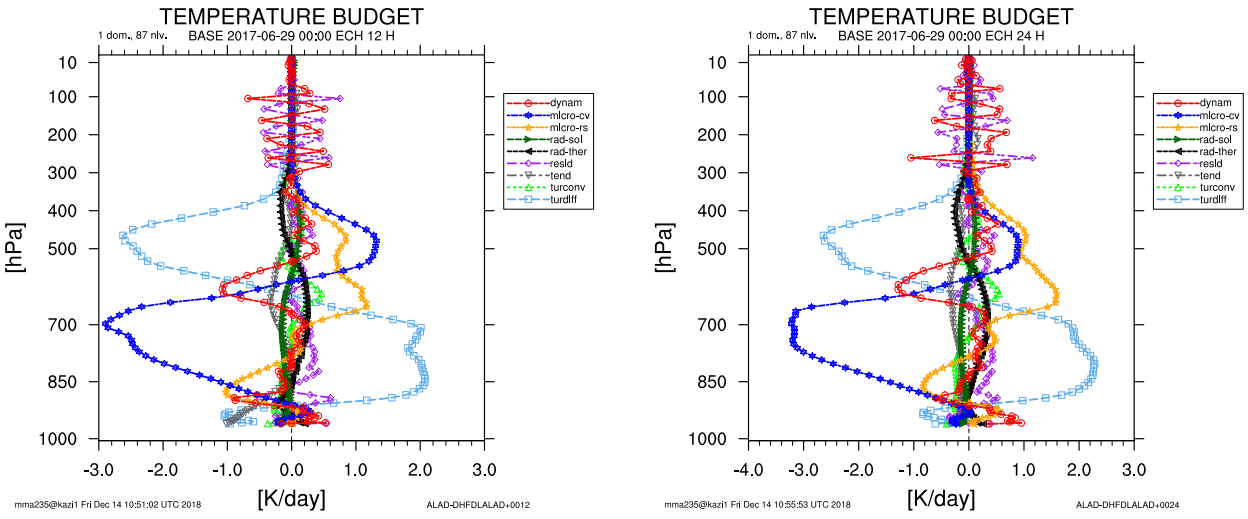

Figure 12: Impact on averaged temperature budget for the summer case at +12 hours (left) and +24 hours (right). "+" sign indicates that particular process is stronger in the reference, while "-" sign indicates that particular process is stronger in the experiment.

Unlike the winter case, where the problems with the upper layer scores appeared around 850 [hPa] pressure level, here the results are mixed and parameter-dependent. Further testing on this subject will be performed after this stay. Here, only in the conclusion part, we will shortly discuss about the potential source of problems in upper layers, as well as about potential solution.

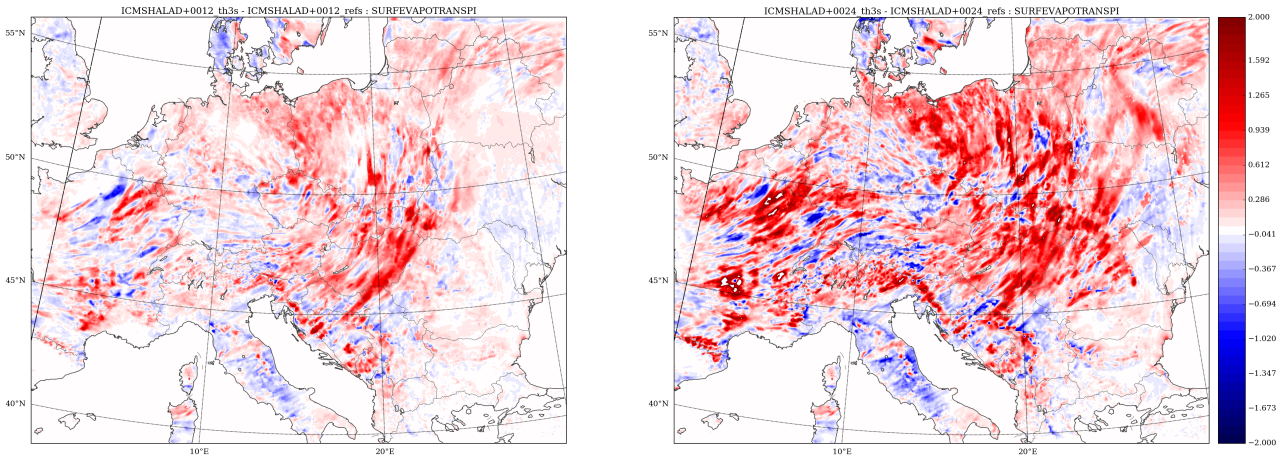

Figure 13: Difference in surface evapotranspiration for the summer case at +12 hours (left) and +24 hours (right). "+" sign indicates that the process is stronger in the experiment, while "-" sign indicates that the process is stronger in the reference.

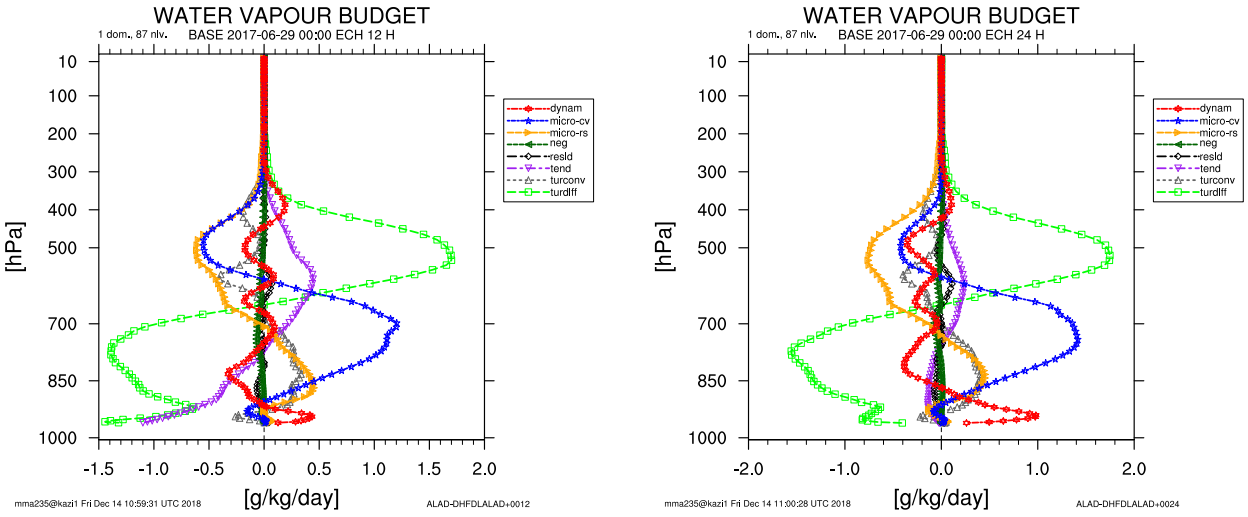

Figure 14: Impact on averaged water vapour budget for the summer case at +12 hours (left) and +24 hours (right). "+" sign indicates that particular process is stronger in the reference, while "-" sign indicates that particular process is stronger in the experiment.

4 Generalization of the BL89 method

There have been many attempts to improve the original BL89 method (e.g. [6], [7], [8] and [3]). Among them, [3] is the most suitable for our environment as it is: i) based on physical principles, ii) vertically adjustable (absolute and relative shear effect) and iii) not expensive (compared to the original) and easy to implement. The new, buoyancy-shear (BS) based length scale (L_{TKE}) is given by:

$$\int_{z}^{z+L_{up}} [\frac{g}{\theta_v(z')}(\theta_v(z') - \theta_v(z)) + c_0\sqrt{e(z)}S(z')]dz' = e(z) \tag{10}$$

$$\int_{z-L_{down}}^{z} [\frac{g}{\theta_v(z')}(\theta_v(z) - \theta_v(z')) + c_0\sqrt{e(z)}S(z')]dz' = e(z) \tag{11}$$

where S(z') is the local vertical wind shear, while c_0 is a constant controlling the magnitude of the shear term. According to authors, the shear term represents the slowdown effect due to vertical decoupling of turbulent eddies (larger eddies are more decoupled) when local shear is strong. It is expected that combined BS scale will better represent local effects in stable stratification, as well as excessive mixing near the neutrality.

In TOUCANS, the BS based length scale is coded as an addition to the "theta2" discretization method. The starting value of c_0 constant is set as proposed in [3], i.e. c_0=0.5. Several diagnostic tests were carried out at the very end of the stay. They pointed out that addition of shear effects to BL89 method may significantly reduce the near-surface mixing, as well as in strong shear zones at higher altitudes. When combined with (desired) local κ scaling, the BS based scale (L_{TKE}) produced slightly higher values of l_m than the global κ scaling version without shear effects. However, the values were still significantly less than those from local κ scaling version without shear effects, which produced relatively poor scores (not shown in the report). The testing will continue from home and/or during the next stay, which is planed for the beginning of 2019.

5 Conclusion and further plans

The new conversion approach from L_{TKE} to l_m is presented here, wherein the near-surface l_m is forced to κz and higher up the L_{TKE} solution prevails. The impact of used averaging operators

on l_m is showed to be small. Regarding the discretization methods, significant impact is seen from the moist one. However, it is not always stable in the prognostic mode.

In general, the pure L_{TKE} solution (local κ scaling) produces too strong mixing above the κz layer and deteriorates the verification scores, especially during the summer convection case. The scores obtained by global κ scaling are much better and near the surface even overcome the reference (for the winter case and partly for the summer). However, the global κ scaling is an equivalent to multiplying the L_{TKE} solution (where it prevails) with some constant. If it is anyhow possible, we would like to avoid this.

One of possible solutions, available in the literature, is to modify the original method by including the shear effects as in [3]. Initial tests showed a good potential when combined with desired local κ scaling. However, this will mostly solve the problem near the surface or, in optimal scenario, up to the level where maximum of l_m is occurred. Analysis of upper level scores showed that we have a degradation of scores around and below the 850 [hPa] pressure level. This is potentially related to sharp transition from κz layer to pure L_{TKE} solution aloft. If it is the case, replacement of min operator by smooth transition from kz layer to L_{TKE} is worth a try.

Finally, the summer case showed us that we will have to take care about the interaction of turbulence with convection. Taking into account how we designed the TKE-based mixing length in TOUCANS, it is likely that we have a problem with large eddies above the κz layer that affect it from aloft. However, this has to be investigated more in detail.

In further work we should:

- Perform detailed testing of generalized BL89 method including: i) calibration of the constant controlling the magnitude of shear term and ii) different averaging operators combined with local κ scaling.
- Develop a method for smoother transition of l_m from κz layer to the aloft layer, where pure L_{TKE} solution prevails. Include the dependency on ABL height.
- Inspect the interaction of turbulence and convection schemes.

Acknowledgment: The author wishes to thank to Jan Mášek and Radmila Brožková for their support and cooperation, as well as to entire ONPP department for their warm welcome and hospitality. This stay is funded by the RC-LACE project.

References

[1] M. Hrastinski. Mixing length computation in TOUCANS. RC LACE stay report, Prague, 14^{nd} May - 8^{th} June 2018.

[2] P. Bougeault and P. Lacarrére. Parameterization of Orography-Induced Turbulence in a Mesobeta-Scale Model. *Mon. Wea. Rev.*, 117:1872–1890, 1989.

[3] Q. Rodier, V. Masson, F. Couvreux, and A. Paci. Evaluation of a Buoyancy and Shear Based Mixing Length for a Turbulence Scheme. *Front. Earth Sci.*, 5:65, 2017.

[4] F. Vana, I. Bastak Duran, and J-F. Geleyn. Turbulence length scale formulated as a function of moist Brunt-Väisälä frequency. *WGNE Blue Book*, chap. 4, 9-10, 2011.

[5] I. Bastak Duran. TOUCANS documentation (15^{th} July version). 2015.

[6] J-C. Golaz, V. E. Larson, and W. R. Cotton. A PDF-Based Model for Boundary Layer Clouds. Part I: Method and Model Description. *J. Atmos. Sci.*, 130:3540–3541, 2002.

[7] E. Sanchez, J. Cuxart, and W. R. Cotton. A buoyancy-based mixing-length proposal for cloudy boundary layers. *Q. J. R. Meteorol. Soc.*, 130:3385–3404, 2004.

[8] G. Lenderink and A. A. Holtslag. An updated length-scale formulation for turbulent mixing in clear and cloudy boundary layers. *Q. J. R. Meteorol. Soc.*, 130:3405–3427, 2004.